Available online at www.sciencedirect.com
ScienceDirect
Deep-Sea Research II 54 (2007) 1949–1965
DEEP-SEA RESEARCH PART II
www.elsevier.com/locate/dsr2

Physical conditions controlling the development of a regular phytoplankton bloom north of the Crozet Plateau, Southern Ocean

Hugh J. Venables*, Raymond T. Pollard, Ekaterina E. Popova

National Oceanography Centre, European Way, Southampton SO14 3ZH, UK

Received 2 October 2006; accepted 25 June 2007

Abstract

A phytoplankton bloom occurs north of the Crozet Plateau annually from September to January. The area, bounded to the north by the Sub-Antarctic Front, is the most northerly of the areas of regular high productivity in the otherwise high-nutrient low-chlorophyll Southern Ocean. Chlorophyll concentrations are at background values to the south and only slightly enhanced over the shallow plateau, producing three contrasting productivity regimes. The CROZet natural iron bloom and EXport experiment (CROZEX) project was aimed at testing the hypothesis that the bloom is caused by natural iron fertilisation from the sediments and islands of the Crozet Plateau. In this paper, the temporal and spatial progression of the bloom and the contrasting productivity regimes are investigated using SeaWiFS and MODIS chlorophyll-*a* (chl-*a*), photosynthetically available radiation (PAR) from SeaWiFS, QuikSCAT wind-stress data, Argo float profiles and data from three research cruises to the region. Comparison of satellite chl-*a* data against *in situ* measurements showed that the satellite data were lower by a factor of approximately 2. Iron, light and grazing are all important in explaining the different productivity regimes. To the north, light is dominant in controlling the timing and location of the bloom initiation, but the spatial distribution of the peak chl-*a* values obtained through the season is associated with the flow pattern and their proximity to the plateau and so are likely driven by nutrient availability. Mixed-layer depths in Argo float density profiles show a shallowing of the mixed-layer depth to the north of $10.8 \pm 1.0\,\mathrm{m\,degree^{-1}}$ across the study area. This gradient, together with a latitudinal gradient in PAR, is sufficient to explain the observed spatial progression of the bloom.

Keywords: SeaWiFS; MODIS; Argo; Sub-Antarctic Front (SAF); Phytoplankton bloom; Mixed-layer depth

1. Introduction

An annual phytoplankton bloom north of the Crozet Plateau is seen in satellite chlorophyll-*a* (chl-*a*) images. The bloom area is bounded to the south by the plateau and to the north and west by the Sub-Antarctic Front (SAF), the furthest north any part of the Antarctic Circumpolar Current reaches (Park et al., 1993; Pollard et al., 2007). The bloom is therefore in the Polar Frontal Zone (Pollard et al., 2002) with macronutrients, including orthosilicic acid (hereinafter silicate) present in non-limiting quantities at the end of winter (Banse,

*Corresponding author. Present address: British Antarctic Survey, High Cross, Madingley Road, Cambridge, CB3 0ET, UK. Tel.: +44 2380 596488.
E-mail address: hjv@bas.ac.uk (H.J. Venables).

0967-0645/$ - see front matter © 2007 Elsevier Ltd. All rights reserved.
doi:10.1016/j.dsr2.2007.06.014

1996). The bloom starts away from the plateau to the north and spreads south towards it. To the south of the plateau chl-*a* concentrations are low, similar to background Southern Ocean levels. Over the plateau itself concentrations are intermediate, despite this area presumably having high nutrient supply from the shallow (mainly <250 m) plateau and small islands (Planquette et al., 2007).

This bloom is in contrast with the high-nutrient low-chlorophyll (HNLC) conditions generally found in the Southern Ocean (Martin et al., 1990; Coale et al., 1996; Johnson et al., 1997; Boyd et al., 1999, 2001). Areas that show increased productivity are around some islands—Kerguelen Islands (Blain et al., 2001), Crozet Islands (this issue) and South Georgia (Atkinson et al., 2001; Korb et al., 2004), frontal regions (de Baar et al., 1995) and marginal ice zones (Moore and Abbott, 2000). In all regions; however, the high concentrations of macronutrients are not fully depleted, with the exception of silicate in some areas, so factors other than macronutrients still control the total annual productivity.

Iron (Martin et al., 1990), light (Mitchell et al., 1991) and grazing (Frost, 1991; Banse, 1996) have been proposed as explanations for the lack of macronutrient utilisation. The first of these has been tested by iron addition experiments (Coale et al., 1996; Boyd et al., 2000), which show that iron is the proximate limiting factor in the study areas chosen as all additions have caused an increase in chl-*a* (de Baar et al., 2005). However, it is most likely that all factors are inter-related (Boyd, 2002). Low light increases iron demand (Sunda and Huntsman, 1997; Maldonato et al., 1999) and low iron drives the phytoplankton community towards smaller, more easily grazed species (Timmermans et al., 2001). When iron is not limiting during *in situ* fertilisation experiments, the peak chl-*a* attained is strongly correlated to the mixed-layer depth (MLD) (de Baar et al., 2005). This could either be due to self-shading effects limiting light availability or the effect of light availability on growth rates since iron addition experiments cause a sudden perturbation to an initially light replete, iron stressed area. This contrasts with naturally iron-fertilised areas where light limitation is lifted in an iron replete area over a longer timescale. These differences may potentially cause significant differences in phytoplankton species composition and grazing rates.

For a large natural iron-fertilised bloom to form associated with an island group it is necessary for there to be both an iron flux from the islands and/or sediments and an area with a sufficient residence time where the iron-enriched water can build up through the winter. The closest equivalents to the Crozet Islands are the Kerguelen Islands and South Georgia. These are also areas with large shallow shelves and islands that significantly affect the flow patterns. Around the Kerguelen Islands it has been shown (Blain et al., 2001; Bucciarelli et al., 2001) that enhanced chl-*a* values are associated with enhanced iron concentrations, but also that both light limitation and grazing significantly influenced the chl-*a* distribution and biomass. Around South Georgia, the physiological condition of phytoplankton indicate that iron fertilisation is one likely cause of high chl-*a* values observed downstream (Atkinson et al., 2001; Korb and Whitehouse, 2004; Holeton et al., 2005), supported by total dissolvable iron concentrations found in shallow shelf waters around South Georgia that are significantly higher than those found offshore (Holeton et al., 2005).

Not all Southern Ocean Islands cause large blooms, for example Prince Edward and Marion Islands (Ansorge et al., 1999) and Macquarie Island (Moore and Abbott, 2000). This could be due to differences in shelf area or different sediment characteristics causing a low iron flux into the surface waters. These islands also have a much less marked effect on the flow pattern and so do not have areas with relatively long residence times where iron can build up through the winter.

The effects of the topography on the flow pattern in the Crozet region are discussed fully by Pollard

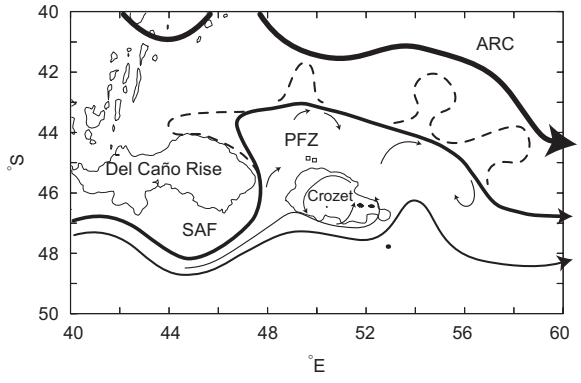

Fig. 1. Schematic of flow around the Crozet Plateau, taken from Pollard et al. (2007). ARC: Agulhas Return Current, PFZ: Polar Frontal Zone, SAF: Sub-Antarctic Front. Dashed lines represent the variability in the path of the flow and small arrows indicate inflows and outflows to the bloom region and the recirculation around the plateau. Faint line is the 2000 m contour.

et al. (2007) and summarised in Fig. 1. Key features relevant to this study are:

(1) The path of the SAF is strongly influenced by bathymetry (Craneguy and Park, 1999; Pollard and Read, 2001). It is initially deflected north or west of north by the Del Caño Rise before retroflecting eastwards and then south-eastwards. This path, together with the plateau to the south, creates a mostly enclosed area with a long residence time, of order 60 days (Pollard et al., 2007).
(2) There are three main flows into the enclosed area—round the eastern end of the plateau, again with flow following the topography; Ekman flux off the plateau, seen in drifter tracks; and detrainment from the SAF seen in drifter and Argo float trajectories and satellite SST and chl-*a* images (Pollard et al., 2007).
(3) Flow close to the plateau is predominantly northwards or a closed circulation around the plateau so that little water that has been close to the plateau flows south.

This provides both an iron flux (Planquette et al., 2007), from the flow close to the plateau, and an area with a long residence time where iron fertilised water can build up over the winter. This is the area in which the bloom forms.

This paper describes and explains the key features of chl-*a* distribution around the Crozet Plateau during austral summer, using satellite chl-*a* data adjusted after comparison with *in situ* measurements. It investigates the spatial progression of the chl-*a* concentrations using MLD calculated from Argo float profiles, photosynthetically available radiation (PAR) and a simple model of phytoplankton growth. It also examines the contrasting productivity regimes north, south and over the plateau.

2. Data

2.1. In situ data

Two consecutive research cruises, D285 and D286, were conducted in the area around the Crozet Plateau (51°E, 46°S) from November 2004 to January 2005 on RRS *Discovery* as part of the CROZEX project (Pollard and Sanders, 2006). The work programme was based around CTD sections/SeaSoar tows, biological stations and underway sampling. Further underway data were collected during the Benthic Crozet cruise D300, again on RRS *Discovery* from December 2005 to January 2006. The causes of contrasting high productivity north of the plateau relative to low productivity to the south, together with its effects on phytoplankton community structure and carbon export, were the focus of CROZEX 2004/2005. The Benthic Crozet study in 2005/2006 examined the effects of contrasting productivity on benthic fauna (Wolff, 2006).

In situ chl-*a* measurements have been used to validate satellite ocean-colour data. Chl-*a* concentrations were determined from water samples collected hourly from the non-toxic ship supply ($\approx$5 m depth) while the ship was in transit, as well as chl-*a* concentrations determined from the 5 m CTD bottle samples. For each sample, 200 ml of seawater were filtered onto a GF/F filter that was then placed in a 20 ml glass scintillation vial and 10 ml 90% HPLC grade Acetone was added for pigment extraction over 24 h in a refrigerator. Chl-*a* concentration was measured using a Turner fluorometer calibrated with a (Sigma) chl-*a* standard (determined on a spectrophotometer), following the Welschmeyer (1994) protocol.

2.2. Remotely sensed data

The remotely sensed data used in this paper are summarised in Table 1. MODIS-derived chl-*a* concentrations (O'Reilly et al., 1998; Feldman and McClain, 2006a) were processed using the standard OC3v1.1 algorithm. SeaWiFS-derived chl-*a* concentrations (O'Reilly et al., 1998; Feldman and McClain, 2006b) were processed using the standard OC4v5.1 algorithm. Datasets used are composites of individual swaths over either 1 or 8 days. The merged SeaWiFS/MODIS product is a composite of these two chl-*a* estimates created by, and available from, the same source. Some ocean-colour data sets included values that were considered unrealistic (up to 50 mg m^{-3}) so the data were filtered. The threshold was set at 15 mg m^{-3} as inspection of images showed coherent high values up to this concentration. SeaWiFS data were used for all comparisons between years, the merged SeaWiFS/MODIS product was used for analysis within 2004. PAR (version 1.2) and Quikscat data were not further quality controlled after being downloaded.

Chl-*a* values approximately follow a log-normal distribution (Campbell, 1995). In this paper the median is used when examining the spatial progression

Table 1
Remotely sensed data used in this study

Sensor	Parameter	Data type and URL	Years
SeaWiFS	Chl-*a*, PAR	Daily and 8 day, 9 km level 3 mapped ⟨http://oceancolor.gsfc.nasa.gov⟩	1997–2006
MODIS	Chl-*a*	Daily, 4 km level 3 mapped ⟨http://oceancolor.gsfc.nasa.gov⟩	2004–2006
SeaWiFS/MODIS merged product	Chl-*a*	Daily and 8 day, 9 km level 3 mapped ⟨http://oceancolor.gsfc.nasa.gov⟩	2004–2006
Quikscat	Wind stress	Daily, 0.25° ⟨http://poet.jpl.nasa.gov⟩	1999–2006
Argo floats	Profiles	⟨http://www.usgodae.org⟩	2002–2006

of the bloom during initiation, as it best describes the bulk of the data. The mean is used for the time series of chl-*a* values throughout the season, as this is used to estimate total productivity (Seeyave et al., 2007) where the small numbers of high values are significant. The median will be very slightly biased high by the small number of outlier values that may have been retained, but the effect is negligible. The mean may be affected more but examination of the 2004 images shows that no significant spikes were included in the calculated time series.

2.3. Argo floats

Argo floats have been present in the area (40–60°S, 40–50°E) since 2002 with the numbers enhanced through 2004–2005 by inflow and deployments from the CROZEX cruises. These data were collected and made freely available by the International Argo Project and the national programmes that contribute to it (www.argo.ucsd.edu, www.argo.jcommops.org). Argo is a pilot programme of the Global Ocean Observing System. The distribution of profiles is close to random in depths of >1000 m. Delayed mode data were used when available. Profiles were rejected if they were flagged as bad data (Gould, 2005) or if they looked suspicious in further manual checking. Of 1303 profiles examined, 180 were rejected. Density was calculated from the temperature, salinity and pressure at each datapoint and then interpolated linearly between datapoints. The mixed layer was taken as the depth where the density difference from the value at 10 m was $0.05\,\mathrm{kg\,m^{-3}}$.

2.4. Definition of boxes used in study

To quantify the temporal and spatial progression of the bloom and investigate the three different areas of productivity, six boxes were defined (Fig. 2). The mean and median chl-*a* values are calculated for each box (and for boxes A and B combined) for each 8-day merged SeaWiFS/MODIS image. The four boxes north of the plateau were chosen to investigate the effect of increasing distance north from the plateau on chl-*a* distribution, and to be away from the edge of the bloom area as the location of the boundary changes with the meandering of the SAF. Box C was set narrower than boxes A and B to study more closely the effects of the edge of the plateau and box D was set to the south-east to study the effects of the two main islands and the flow around the eastern end of the plateau. Further boxes over the plateau (box E) and to the south (box F) were used to study the other two productivity regimes. Boxes A and B have been combined to characterise the regime north of the islands for comparison with the areas of these last two boxes.

3. Results and discussion

3.1. Comparison of ocean-colour images with in situ data

For each of the 810 *in situ* chl-*a* measurements collected during the three cruises, the value from the corresponding individual pixel of the ocean colour image of the day of collection was recorded, if the pixel was cloud free.

This resulted in 224 pairs of *in situ* and satellite data for the merged SeaWiFS/MODIS product. Four outliers were removed, which were caused by either very small-scale patchiness in chl-*a* that was poorly represented by a 9×9 km pixel (such areas were targeted on D285 and D286) or by a series of bad *in situ* values. The remaining data span a range of *in situ* values up to $2.7\,\mathrm{mg\,m^{-3}}$ and are shown in

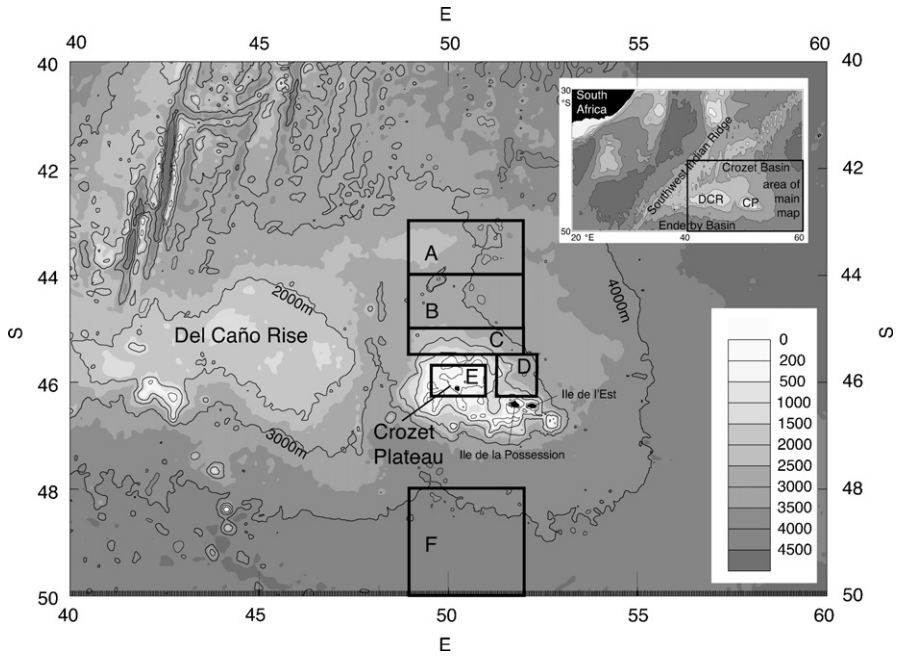

Fig. 2. Location of the boxes used to characterise the progression of the bloom, over the topography of the area (Sandwell and Smith, 1997). The position of the Crozet Plateau is also shown, inset, relative to South Africa.

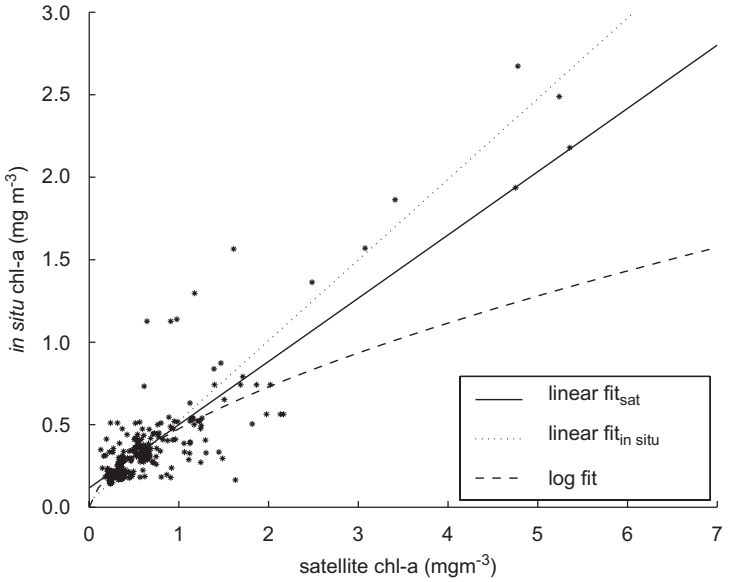

Fig. 3. Merged SeaWiFS/MODIS chl-*a* against *in situ* chl-*a* values. Linear fit_{sat} is the regression line for satellite values regressed onto *in situ* values (for comparison with other studies), the log fit (transformed back for linear axes) has been calculated this way round. Linear $\text{fit}_{\text{in situ}}$ is the regression line for *in situ* values regressed onto satellite values, as is needed to adjust satellite values to our best estimate of *in situ* values.

Fig. 3. The least squares regression fits, with 95% confidence intervals are:

$$\text{CHL}_{\text{merged}} = 0.12 \pm 0.04 + (0.38 \pm 0.03) \times \text{CHL}_{\text{in situ}}, \quad r^2 = 0.78, \tag{1}$$

$$\text{CHL}_{\text{in situ}} = -0.08 \pm 0.08 + (2.05 \pm 0.15) \times \text{CHL}_{\text{merged}}. \tag{2}$$

The same process with just SeaWiFS data produced 113 *in situ* and satellite data pairs as described

above, again with a maximum *in situ* value of $2.7\,mg\,m^{-3}$. After the same removal of outliers, the relationships

$$CHL_{SeaWiFS} = 0.13 \pm 0.05 + (0.39 \pm 0.03) \times CHL_{in\ situ}, \quad r^2 = 0.85, \tag{3}$$

$$CHL_{in\ situ} = -0.15 \pm 0.12 + (2.21 \pm 0.18) \times CHL_{SeaWiFS}, \tag{4}$$

were found. In both cases, removing the outliers did not significantly affect the gradient or intercept of the relationships but did increase the correlation coefficient from approximately 0.6 and narrowed the confidence intervals.

Although 118 such data pairs were found for MODIS, they did not span a wide range of *in situ* values ($\leqslant 1.4\,mg\,m^{-3}$) and so satellite data from ± 1 day also were included, if a match was not found for the same day. This produced 240 data pairs and increased the number of high *in situ* values, but the range was still similar to before. The relationships

$$CHL_{modis} = 0.17 \pm 0.04 + (0.32 \pm 0.04) \times CHL_{in\ situ}, \quad r^2 = 0.52, \tag{5}$$

$$CHL_{in\ situ} = 0.06 \pm 0.09 + (1.64 \pm 0.20) \times CHL_{modis} \tag{6}$$

are different from those found for SeaWiFS, indicating that MODIS estimates are higherthan SeaWiFS, at least at low ($<1.5\,mg\,m^{-3}$) values. This is also found by comparing the two products in low-productivity water south of the islands:

$$CHL_{SeaWiFS} = 0.042 \pm 0.003 + (0.79 \pm 0.020) \times CHL_{modis}, \tag{7}$$

but taking data from the whole area there is a close match:

$$CHL_{SeaWiFS} = -0.022 \pm 0.008 + (1.07 \pm 0.015) \times CHL_{modis}. \tag{8}$$

This gives confidence in using the merged product in this area though the extra coverage is at the loss of some consistency due to the two different data sources.

The linear fits are significantly influenced by the few high values found in the SeaWiFS match-ups. To check the relationship for the merged SeaWiFS/MODIS product the data were log transformed and a least squares fit found to those datapoints. The result, transformed back to a linear scale, shows good agreement with the original linear fit at low chl-*a* values, but deviates from the datapoints and linear regression line at high values (Fig. 3). Therefore the linear fit of Eq. (2) has been used, together with the merged SeaWiFS/MODIS product, to study the bloom in 2004/2005. SeaWiFS data have been used back to 1997 and they have been similarly adjusted, using the same equation for consistency (it falls within the confidence intervals for the SeaWiFS comparison). The linear nature of this adjustment means that original data values can be recovered and all trends and patterns are independent of the adjustment. This adjustment is purely empirical and does not represent a correction to the satellite algorithms, but it is necessary if the time series of chl-*a* values, together with other cruise data, are to be used to study productivity at larger time and space scales than was possible from the ship alone.

The Southern Ocean is recognised as an area where satellite ocean colour derived chl-*a* estimates differ significantly from *in situ* measurements (O'Reilly et al., 1998; Moore et al., 1999; Gregg and Casey, 2004; Holm-Hansen et al., 2004; Korb et al., 2004). The linear relationship we found is similar to that found by Korb et al. (2004) and Dierssen and Smith (2000) and best suited our data set, in large part because of the sensitivity of a log/log fit when there is considerable scatter in the data. The differences between the relationships found in this study,

$$CHL_{SeaWifs} = 0.13 \pm 0.05 + (0.39 \pm 0.03) \times CHL_{in\ situ}, \quad r^2 = 0.85, \tag{9}$$

compared to that found from around South Georgia,

$$CHL_{SeaWifs} = 0.30 + 0.28 \times CHL_{in\ situ}, \quad r^2 = 0.61, \tag{10}$$

(Korb et al., 2004) are largely due to the higher *in situ* values in the latter data set. The SeaWiFS values for these are generally lower than the regression line that would fit the rest of the data (see Fig. 3 in Korb et al., 2004) and so cause the gradient of the regression line to be lower and the intercept higher. This is either due to SeaWiFS underestimating high values most significantly, for which there is some evidence in Gregg and Casey (2004), or the use of 8-day images in the South Georgia study that are less likely to capture high values due to advection, temporal changes in chl-*a* concentrations and dilution from mixed-layer deepening events.

3.2. Spatial and temporal progression of the phytoplankton distribution

3.2.1. Merged SeaWIFS/MODIS chl-a images

Fig. 4 shows 6 weekly merged SeaWiFS/MODIS images from 2004, after applying the above adjustment (Eq. (2)). The first cruise, D285, arrived in the area on 9 November 2004, just after the peak of the bloom. The areas north and south of the plateau and the plateau area itself form three distinct regimes of differing productivity patterns that have to be described and explained separately, these are described in points 1–3 below. The images have been selected to show the main features of the temporal and spatial progression of the bloom.

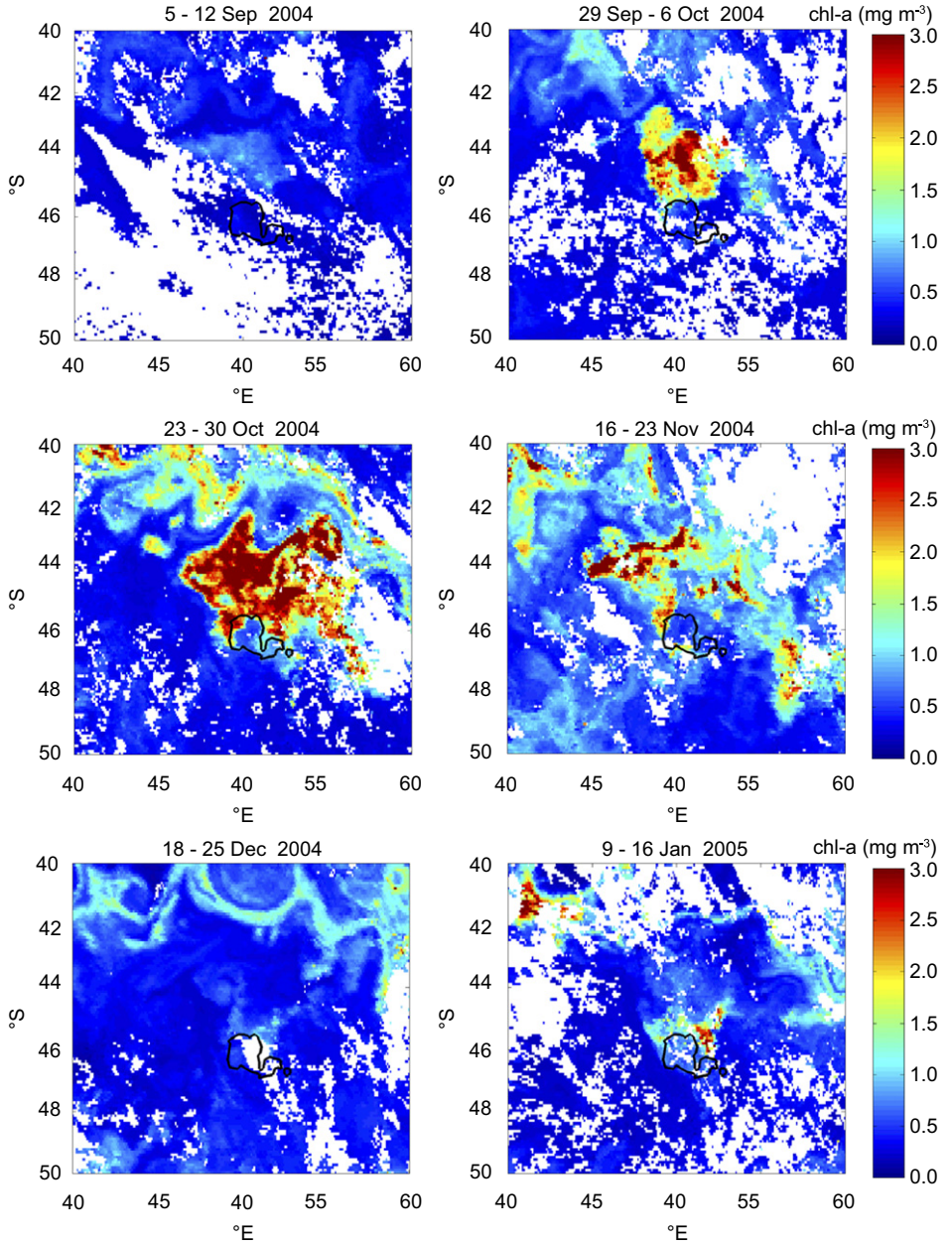

Fig. 4. A selection of 8-day merged SeaWiFS/MODIS chl-*a* images through the season showing the development, spatial extent, north-south contrast and persistence of the bloom around the plateau. The black line is the 1000 m contour, marking the edge of the steep sided plateau.

(1) High chl-*a* concentrations (1.5–8 mg m^{-3}) to the north of the plateau. The bloom starts in early–mid September with enhanced chl-*a* concentrations initially separated from the plateau by a strip of low chl-*a* waters, approximately 100 km wide (Fig. 4A). The bloom then spreads south across this strip (Fig. 4B) and finally south-east towards the two main islands (Fig. 4C).
(2) Low chl-*a* concentrations (0.2–0.5 mg m^{-3}) to the south of the plateau (Figs. 4B–D). These values show no increase over concentrations upstream to the west, indicating little effect from the islands. The high values to the south-east in Fig. 4D are downstream of the bloom. This contrast each side of the plateau is visible in SeaWiFS images at this time of year (September–December) back to 1997 (beginning of the SeaWiFS mission). The contrast with the north is most likely due to flow consistently advecting island influenced (iron enriched) water to the north (Pollard et al., 2007; Planquette et al., 2007).
(3) Low to medium (0.2–1 mg m^{-3}) chl-*a* concentrations over the plateau itself, despite this area presumably having the highest nutrient concentrations. However, we could not confirm this as we were unable to take the ship into this shallow and poorly charted area, although high iron concentrations were found immediately north of Ile de la Possession (Planquette et al., 2007).
(4) The bloom is bounded to the west and north by very low chl-*a* concentrations in the SAF and this separates it from increased concentrations further north associated with the Sub-Tropical Front and Agulhas Return Current. These contrasts show the strong meanderings in these fronts. Water exchange between the SAF and the bloom area increases the chl-*a* concentration in the SAF downstream to the east as iron-enriched water is entrained into the front from the bloom area.
(5) Two inflows into the bloom area can be seen. Water with low iron concentrations separates from the SAF and enters the bloom area, causing the patches of low chl-*a* in the western side of the bloom (Fig. 4C). Water also flows around the eastern end of the plateau, causing a further area of low chl-*a* values (Fig. 4B) due to HNLC water entering the area from the south characterised by deeper mixed layers and/or low iron.
(6) Anticyclonic flow around the plateau described in Pollard et al. (2007) advects chl-*a* southwards around the western side of the plateau (Figs. 4B–D).
(7) Chl-*a* concentrations reduce rapidly in the bloom area during November (Fig. 4E), but increase again just north of the plateau in January, due probably to a re-supply of iron from the islands and plateau (Fig. 4F).

Although satellite ocean-colour imagery provides a good indication of spatial contrasts in phytoplankton abundance, they may not provide a representative impression of the contrast in absolute biomass. One reason is that chl-*a* per cell is higher in areas of high iron concentration, as seen in several iron addition experiments (de Baar et al., 2005), with as much as a four-fold increase in chl-*a*:carbon observed at the surface (Landry et al., 2000). This effect is due to the iron requirements of photosynthetic units that also contain chl-*a* (Sunda and Huntsman, 1997). Deeper mixed layers found to the south will also lead to greater mixed-layer integrated biomass per unit surface chl-*a*, if all other factors are equal.

Despite the problems with chl-*a* to biomass ratios, satellite calibration in the Southern Ocean and cloud cover (luckily insignificant in this study), satellite chl-*a* images are still very valuable for observing chl-*a* distributions over large time and space scales. Without it, the original hypothesis for studying the Crozet region would not have been formed. Most importantly, the images allow the progression of the bloom to be characterised, both over the 9 years for which data are available, and also for 2004/2005 in particular, allowing us to set the findings from our cruise in context of the bloom, which preceded our arrival at the study region.

3.2.2. *Temporal progression*

Fig. 5 shows the mean chl-*a* north (boxes A and B combined), south (box F) and over the plateau (Box E). Mean rather than median values were used so that total seasonal productivity could be estimated in these areas (see Seeyave et al., 2007). The progression in each area is discussed separately.

3.2.2.1. North of plateau. North of the plateau, the increase in chl-*a* is approximately exponential through August–October. Following their collapse, chl-*a* concentrations increase again to greater than pre-bloom concentrations close to the islands at the

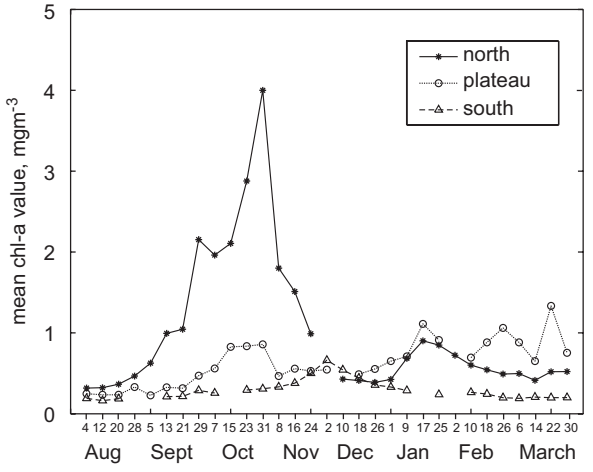

Fig. 5. Time series of mean chl-*a* for 2004 after adjustment. Missing points are due to >80% cloud cover over the box in the 8-day images.

eastern end of the plateau and along the whole of the northern edge at lower concentrations (Fig. 4F). This is consistent with a source of iron that stimulates biomass and productivity from the eastern islands, together with a weaker source from the shallow plateau, vertical mixing along the edge of the plateau or advection of iron by the circulation around the plateau. An iron source has been confirmed from the eastern islands (Planquette et al., 2007). Moore et al. (2007) found iron to be the proximate limiting nutrient in all areas during on-deck incubation experiments carried out after the bloom peak, but with light exerting a secondary effect. Downstream of the bloom area, at 46°S 65°E in January–February, Sedwick et al. (2002) also found, in similar ship-board experiments, that iron was the proximate limiting nutrient, with silicate exerting a secondary control. These findings all indicate that the initial decline in bloom chl-*a* concentrations was due to iron limitation, but not withstanding the potential for grazing controls (Fielding et al., 2007). Close to the Polar Front, Abbott (2000) found a similar pattern, with the bloom starting as light limitation is lifted and then the peak being controlled by nutrient limitation and/or by grazing.

3.2.2.2. Over the plateau. Over the plateau, nutrients including iron, should be at their highest concentrations due to supply from the shallow plateau (much of it <250 m deep) and several small islands, since an iron source has been identified from Ile de la Possession (Planquette et al., 2007). However, chl-*a* increases only to a low peak ($<1\,mg\,m^{-3}$ in 2004 being typical of the 1997–2005 period) before declining and fluctuating around that concentration (Fig. 5). This low peak is inconsistent with the probability that both iron and macronutrients were non-limiting, so that some other limiting mechanism must be in place.

One explanation is that tidal and mean flows over the shallow topography may lead to enhanced mixing at the base of the water column, which could merge with the surface mixed layer. If so, this could lead to very deep mixed layers (>150 m) which would exert light limitation on the phytoplankton community. Furthermore, the water also could be turbid due to suspended sedimentary material, further reducing light availability. The possibility of the water being turbid also makes the satellite chl-*a* values less reliable, but it is more likely that they would be biased high by suspended particles in the surface waters (International Ocean-Colour Coordinating Group, 2000), so it is unlikely to be the cause of the significant difference between this area and north of the plateau.

Grazing control also may be a dominant influence. This could occur over the plateau due to a greater standing stock of zooplankton overwintering in the shallow shelf waters. Studies at the nearby Kerguelen Islands found counts of a neritic species (*Drepanopus pectinatus*) in a coastal bay that were 2 orders of magnitude higher than counts of copepods at an offshore site (KERFIX) in winter (Razouls et al., 1996; Razouls et al., 1998). *D. pectinatus* is common also to the Crozet Plateau (Fielding et al., 2007) and has a similar distribution characterised by near-shore abundance and scarcity offshore. As *D. pectinatus* can respond rapidly to changes in chl-*a* concentration, reaching peak growth rates of $0.10\,day^{-1}$ (Alonzo et al., 2003), grazing control by this species may be substantial and is consistent with the fluctuating pattern (period $\approx$30 days) in chl-*a* concentrations seen later in the season (Ryabchenko et al., 1997).

Nevertheless, as *Discovery* could not sample within the shallow plateau region because of uncharted bathymetry, all hypotheses regarding controls on chl-*a* biomass here remain speculative.

3.2.2.3. South of plateau. The area to the south of the plateau is mostly 'upstream' of the plateau, since the dominant flow patterns in the region of the plateau are northwards or a closed circulation around the plateau (Pollard et al., 2007), so it is

expected that this area will receive little or no iron supply from the shallow plateau, as confirmed by Planquette et al. (2007). There is also a less favourable light climate as the mixed-layer deepens to the south by 11 m degree^{-1} on average, described in Section 3.3.1. This reduces phytoplankton growth rates (Seeyave et al., 2007) and increases iron demand (Sunda and Huntsman, 1997). The productivity regime is therefore similar to the open ocean areas of the Polar Frontal Zone between the Polar Front and SAF (Banse, 1996; Moore et al., 1999).

There is a well-defined, but low, peak in chl-*a* values at the beginning of December, prior to maximum light availability, indicating that the area is not light limited at the time of peak chl-*a* concentrations. After this, chl-*a* values are consistently low south of the plateau, either indicating tight grazing control or nutrient limitation. Low V_{NO_3} day^{-1} rates in the southern HNLC region (Lucas et al., 2007) and positive phytoplankton responses to iron additions (Moore et al., 2007) indicate that iron limitation is strong, although grazing pressure was also found to be high in the area (Fielding et al., 2007) during the second leg of the cruise in December–January. The increase in grazing pressure to the south may be due to the fact that slower phytoplankton growth rates allow zooplankton populations time to respond to available food and to effectively control phytoplankton biomass. The consistency of the low chl-*a* values also indicate that there is probably no significant resupply of iron during the summer, nor indeed over winter, as confirmed by Planquette et al. (2007).

Table 2
Week after 4 August that the median chl-*a* value in each box north of the plateau reached 1 mg m^{-3} after adjustment (see Fig. 5 for actual dates)

Year	Box			
	A	B	C	D
1997	7	7	7	12
1998	5	6	6	8
1999	8	9	11	11
2000	7	8	10	14
2001	12	13	14	15
2002	8	9	9	9
2003	9	11	11	12
2004	7	7	8	10
2005	11	8	8	7
Mean:	8.2	8.7	9.2	10.9

Table 3
Seasonal maximum of the weekly median chl-*a* (mg m^{-3}) in each box from adjusted merged SeaWiFS/MODIS chl-*a* data

Year	Box					
	A	B	C	D	E	F
1997	1.59	3.69	5.63	4.56	1.35	0.43
1998	2.59	3.10	5.44	8.13	0.80	0.35
1999	2.69	6.71	5.63	7.45	2.33	0.59
2000	1.31	1.81	3.38	8.27	0.77	0.45
2001	1.17	1.78	4.11	3.32	0.59	0.45
2002	1.63	2.50	3.21	5.25	4.11	0.69
2003	2.25	2.33	2.33	2.88	0.77	0.36
2004	3.10	3.10	2.88	2.50	0.70	0.64
2005	3.21	2.50	4.25	4.40	0.90	0.41
Mean:	2.17	3.06	4.10	5.20	1.37	0.49

3.2.3. Spatial progression

As has been noted from the series of chl-*a* images (Fig. 4) the bloom progression in 2004 is southwards, starting well north of the plateau, then spreading south towards the plateau, and finally towards the eastern side, close to of the islands. This pattern is consistent for most years, as shown by Table 2. This shows in the first week (with week 1 starting on 4th August, see Fig. 5 for other dates and note that 'week' here is used for the 8-day periods of satellite composites) that median chl-*a* values in each box (defined in Fig. 2) reached 1 mg m^{-3}, a value indicating the start of bloom development. Except for 2005, week increases from boxes A to D—showing a clear and significant trend of the bloom developing later to the south. The delay between boxes A, B and C is 4–7 days degree^{-1}. As is demonstrated and discussed later (Section 3.3.3), this can be explained by considering the gradient in the mixed layer and incoming irradiance, showing that the bloom is initially predominantly light limited.

In a light-limited system, where all other factors are non-limiting, the highest surface chl-*a* values are likely to occur where the light climate is best. Table 3, however, shows that maximum chl-*a* values generally increase towards the plateau, whereas the MLD deepens towards the plateau, as shown later (Section 3.3.1).

It has been argued above that the chl-*a* decline north of the islands is due to nutrient limitation and the gradient in the magnitude of the peak is also likely to be due to the differing nutrient supply

between the two main inflows into the bloom region. Water entering the area by detrainment from the SAF, described in Pollard et al. (2007), has had little contact with the plateau so will have approximately background concentrations of iron but high silicate due to its Sub-Antarctic origin. Water that flows around the plateau and enters the region close to the eastern islands, or via Ekman flux from over the plateau, will likely become fertilised with iron. The proportion of water that has detrained from the SAF will increase to the north and west as distance from the front decreases and distance from the plateau increases and this could create a gradient in iron, with concentrations decreasing with distance from the plateau (see also Planquette et al., 2007). The numbers of a neritic zooplankton species, *D. pectinatus*, reduce with distance away from the plateau (Fielding et al., 2007), supporting the concept of dilution of island-influenced water away from the plateau. The peak chl-*a* being driven by iron rather than light is contrary to the findings of de Baar et al. (2005), where peak chl-*a* concentrations for different iron enrichment experiments were driven by the light climate.

3.3. Mixed-layer depth variations and phytoplankton growth

3.3.1. Mixed-layer depth gradients

To investigate factors controlling the initialisation of the bloom, the MLD was diagnosed from 838 Argo float profiles within 40–60°E, 43–50°S. To remove the seasonal effect on MLD, a sinusoidal plot, as a function of day of year, was fitted to the data (Fig. 6) and residuals were calculated from this. Although MLD in any given place do not follow a sinusoidal curve, it was found to be a good fit to the data, which come from a large spatial area over 5 years. MLD recorded in winter are in the range 100–250 m south of the plateau, north of the plateau they are mostly in the range 75–150 m. Due to the coarse sampling of Argo floats, maximum winter mixing depths are likely to be greater than these values. In summer, MLD are 40–100 m south of the plateau while those north of the plateau are mostly under 60 m.

There is a northwards reduction in the residual MLD of $10.8 \pm 1.0\,\mathrm{m\,degree^{-1}}$ latitude (Fig. 7). There is no significant difference between the latitudinal gradient in winter and summer. When only data from north of the islands during the time

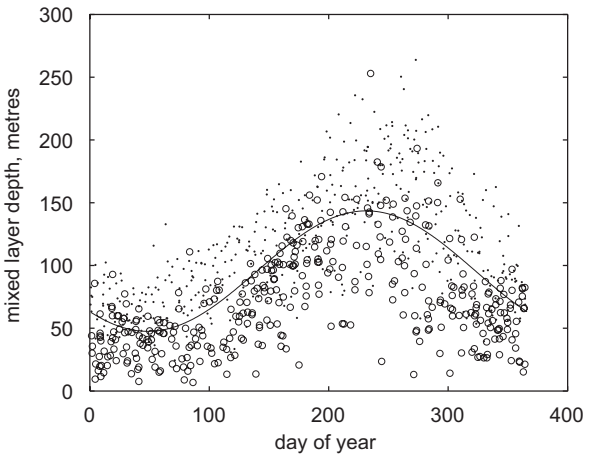

Fig. 6. Mixed-layer depth from Argo floats from 43 to 50°S, 40–60°E against day of year. A sinusoidal fit has been used to approximate the yearly trend and so allow effects of latitude to be investigated. Open circles are for profiles north of the plateau, dots for those south of the plateau.

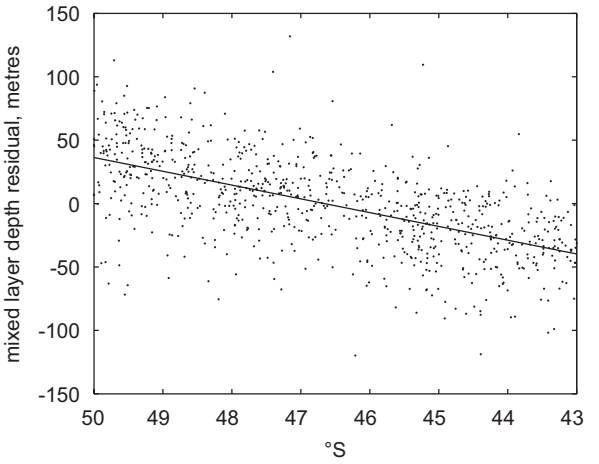

Fig. 7. Residual mixed-layer depths, after effects of time of year have been removed. With least squares regression line.

period of the bloom (September–February) are used, the gradient is similar: $11.3 \pm 3.8\,\mathrm{m\,degree^{-1}}$ latitude (211 profiles). This relates to a deepening, on average, of 30 m across the bloom and 50 m between north and south of the plateau.

The MLD, in a given location, will decrease rapidly from deep winter levels to shallow summer values. The timing of this shoaling depends on atmospheric forcing, which will vary over large spatial scales relative to the bloom area, and the existing density profiles, which vary little within water masses but change rapidly over small spatial

scales between water masses. Argo float profiles indicate that this re-stratification event occurs earlier to the north, but exactly by how much is not reliably known. Consequently, Section 3.3.3 assumes that re-stratification occurs simultaneously across the bloom area and that the gradient in MLD is constant in time.

3.3.2. Source of gradients

Two main inputs into the bloom area that control the nature of the vertical density profiles near the surface are the source of inflowing water and surface buoyancy fluxes. It is clear that there is inflow of water into the area of Sub-Antarctic origin (Pollard et al., 2007). Mixing across the SAF also may be important, especially as the very sharp temperature and salinity gradients in the area imply a relatively low volume flux may have a significant effect.

Fig. 8 shows that increases in surface temperatures in the region 43–46°S are associated with low salinities despite both temperature and salinity increasing across the SAF. This shows that cross-frontal mixing is not a significant source of water to the bloom area. The lower panel shows a constant temperature and salinity at 200 m south of the SAF, again indicating a lack of mixing. It also indicates that higher surface temperatures will be associated with greater density stratification. This also means that water originating from north of the SAF does not need to be considered as an iron source for the bloom area.

Observed gradients in MLD therefore must be due to *in situ* forcing through buoyancy fluxes and wind stress. It is not possible to create a complete buoyancy budget for the region at the required resolution, but NCEP data (not shown, from their website: http://www.cdc.noaa.gov/) show that there is a downward trend in precipitation and no trend in evaporation between August and November. Freshwater fluxes are therefore not driving temporal changes in stratification. There is also no significant difference between 42.9 and 44.8°S in either variable.

PAR data from SeaWiFS, which is strongly correlated to total incoming irradiance, show significant spatial and temporal gradients (Fig. 9) of approximately 1 Einstein m^{-2} day^{-1} $degree^{-1}$ and 1/3 Einstein m^{-2} day^{-2}, respectively. Most of the density difference is due to heating, which agrees with the strong gradients in heat flux rather than freshwater flux. Gradients in PAR will also affect phytoplankton directly through varying light intensity in the mixed layer. Wind stress also shows latitudinal gradients across the area, increasing to the south (Fig. 9) and therefore further contributing to the observed gradient in MLD. The decrease in

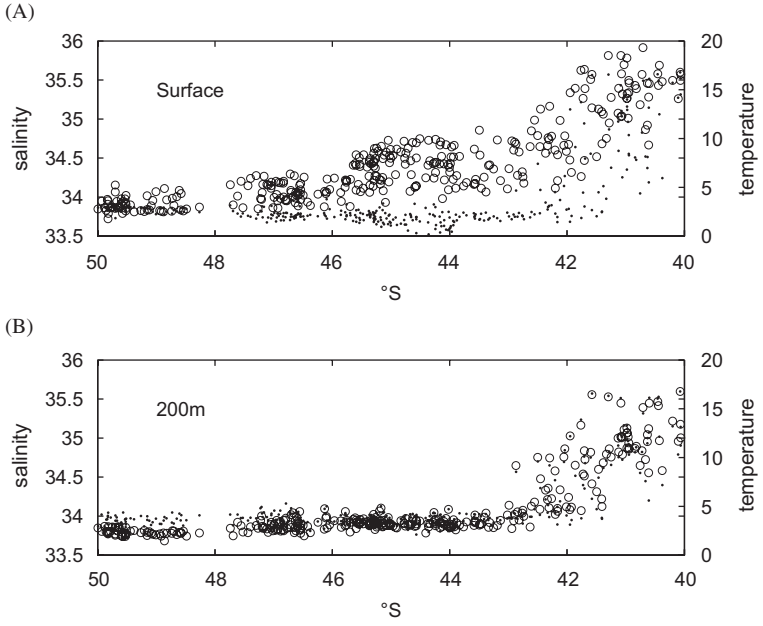

Fig. 8. Temperature and salinity from Argo float profiles at the surface (above) and 200 m (below) from region 40–50°S, 47–52°E. Open symbols represent temperature, points represent salinity.

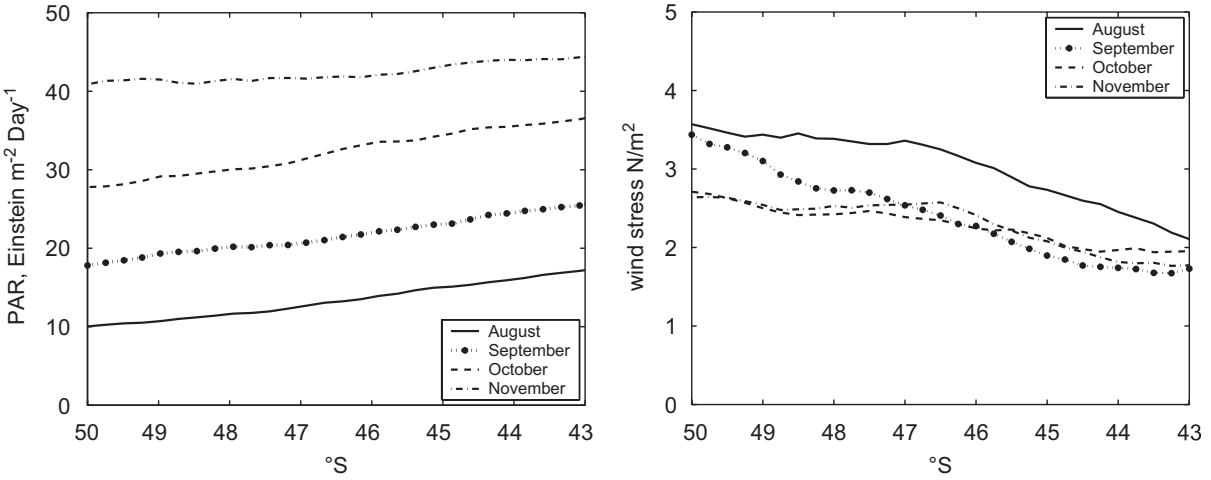

Fig. 9. Plots of monthly incoming irradiance and wind stress for 2004.

wind stress between August and September acts to allow re-stratification of the surface water column.

Lateral mixing timescales for the area north of the Crozet Plateau are important for the bloom that forms there. These can be assessed directly using float tracks (Pollard et al., 2007) which gives a timescale of 100 days at 1000 m. Information also can be inferred from the mixed-layer gradient and the bloom itself. For the gradient in the mixed layer to develop, the seasonal heating that creates it must act over a shorter timescale than the lateral mixing, as this will act to erode the gradient. This suggests that 100 days is also valid closer to the surface than 1000 m. As drawn-down nutrients must be re-supplied between each annual bloom, the lateral mixing timescales also must be less than or similar to 1 year. However the reduction in the peak chl-*a* values with increasing distance from the plateau indicates that lateral mixing does not create a homogenous initial nutrient field. This could be because the mixing timescale is more than a year, but the effect is at least partly due to water with low iron concentrations detraining from the SAF and diluting the iron-enriched water from close to the plateau.

3.3.3. *Effects of gradients in mixed-layer depth and incoming irradiance on phytoplankton growth rates*

The observed gradient in MLD ought to produce increasingly favourable conditions for phytoplankton growth with distance north, assuming non-limiting nutrient availability, including iron. If so, this should lead to chl-*a* concentrations increasing more rapidly to the north. To test this hypothesis, a simple model of phytoplankton growth was used with differing inputs to represent the effects of 1° changes of latitude. Growth is represented by

$$\frac{dC}{dt} = f(h, I)C, \tag{10}$$

where C is the chl-*a* concentration, h is the MLD, I is surface PAR, and t is time. It is assumed that there is rapid re-stratification after winter mixing so that the MLD reduces suddenly and simultaneously across the entire bloom area. Therefore h is subsequently a constant in time. Conditions are considered to be solely light limited, so growth rate, f, is defined as the maximum phytoplankton growth parameter, κ, multiplied by the average irradiance over the MLD. The diffuse downwelling attenuation coefficient, K_d, is a function of the chl-*a* concentration to allow for self-shading, using the relationship found during the cruise:

$$K_d = 0.04 + 0.063 \times (C^{0.38}). \tag{11}$$

The temporal increase in PAR is included by setting α as 0.3 Einstein m^{-2} day^{-2}.

$$f(h, I) = \frac{\kappa I}{h}\left(\frac{1 - e^{-K_d h}}{K_d}\right), \tag{12}$$

$$I = I_0 + \alpha t. \tag{13}$$

The initial equation then must be solved numerically. An initial value C_0 of 0.33 was used to match the satellite data and κ was set at 0.0085 m^3 $Einstein^{-1}$ so that it took approximately 32 days for C to

increase from C_0 to 1 mg m^{-3} for a mixed layer of 50 m, to fit the timescale found in satellite images.

The model was used to test the effect of 1° of latitude on the time taken for chl-*a* to increase to 1 mg m^{-3}. To do this, h and I_0 were set at 40 m and 11 Einstein m^{-2} day^{-1}, respectively and for further paired values of 50 m and 10 Einstein m^{-2} day^{-1} and 60 m and 9 Einstein m^{-2} day^{-1} to account for observed latitudinal gradients in MLD and insolation. The results are shown in Fig. 10.

The time taken for the chl-*a* to reach 1 mg m^{-3} increased by approximately 6 days degree^{-1} of southward progression (Fig. 10), which is in good agreement with the average progression of 4–7 days degree^{-1} found in the satellite data between boxes A and C. This shows that physical conditions (i.e., light and MLD) control the southwards progression of the bloom, where the variation in MLD had a greater influence than the variation in insolation, though the latter was not negligible.

The observed difference between boxes C and D is 21 days degree^{-1}, where the extra delay is consistent with northerly flow of water into that area, with deeper stratification typical of water from further south. Evidence of this flow can often be seen as a tongue of cold water in SST images (Pollard et al., 2007). Nevertheless, a bloom does eventually form and persist there, indicating that water becomes iron fertilised as it reaches the area just north of the islands.

This study and that of Planquette et al. (2007) confirm that the Crozet bloom was initiated by increased light in an area already enriched with iron over the winter period. This contrasts with artificial iron enrichment experiments (e.g. SOIREE, Boyd et al., 2000) where iron was added to an area with a favourable light climate. The similarities and differences observed between the Crozet bloom and such artificial iron enrichment experiments can therefore be used to help assess the impacts of increased iron supply to currently iron-limited areas.

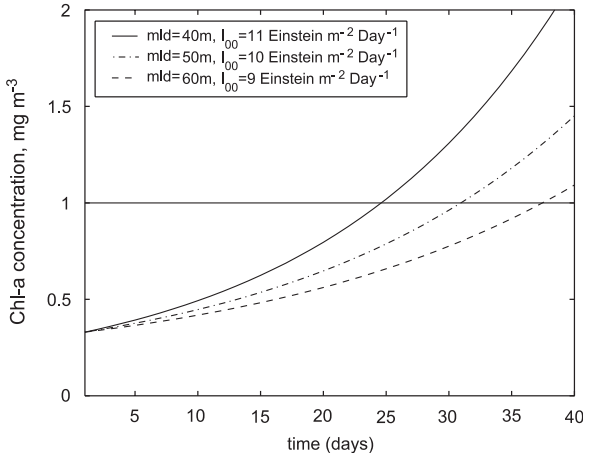

Fig. 10. Modelled variation in chl-*a* increase with different mixed layers and insolation after a sudden stratification. The 10 m and 1 Einstein m^{-2} day^{-1} steps represent the effects of 1° of latitude in average mixed-layer depth and incoming irradiance.

3.3.4. *Strength of the pycnocline*

Arguments presented so far rest on the relationship between light and MLD. Clearly then, it is important to consider how robust the MLD is as a function of pycnocline strength and to further consider what implications this may have on phytoplankton.

The density difference between the mixed layer and 50 m below the bottom of the mixed layer also increases to the north, as shown by Fig. 11. Equivalent differences in temperatures and salinity (not shown) show that surface heating dominates density differences, and as heating is strongest in the north, it will lead to less variable and shallower MLD. This will allow phytoplankton within the mixed layer to develop in a more consistent and higher light environment with consequently reduced losses due to mixing and re-stratification events. This further enhances the ability of phytoplankton to develop earlier in the north of the bloom area, although there, the vertical resupply of nutrients to the surface through mixing will be reduced. This is consistent with observations of enhanced chl-*a* concentrations persisting close to the plateau, but

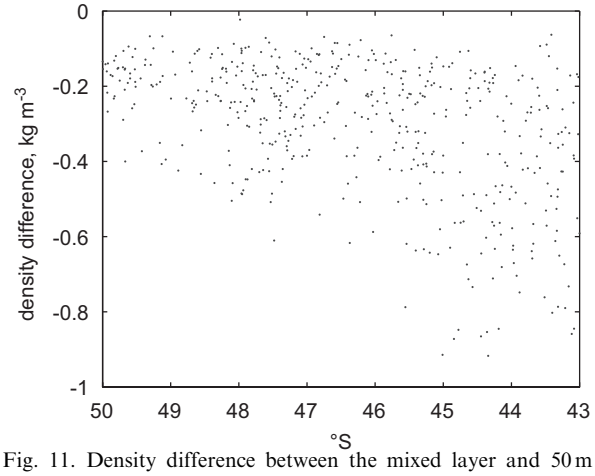

Fig. 11. Density difference between the mixed layer and 50 m below the mixed layer.

not further north, though this will largely be due to the proximity of the plateau, which provides a source of nutrients.

4. Conclusions

Chl-*a* estimates from SeaWiFS and MODIS are both approximately half the measured *in situ* values. After correcting for this, satellite chl-*a*, irradiance, and wind-stress data, together with Argo float profiles can be used to describe and explain the spatial and temporal distribution of phytoplankton around the Crozet Plateau.

The combination of the hydrography and bathymetry creates three distinct productivity regimes. North of the plateau is downstream of the islands and shallow shelf so the area is iron enriched and has very high productivity, atypical of the Southern Ocean. South of the plateau is upstream of the iron source and has considerably deeper mixed layers and much lower productivity, typical of the HNLC conditions in the Southern Ocean. The area above the shallow plateau appears to be grazing controlled, probably due to enhanced over-wintering and rapid growth rates of neritic *D. pectinatus* in the shallow water and around the islands.

The bloom forms to the north of the plateau in an area with a high residence time, which allows iron-fertilised water to accumulate during the winter. It also allows latitudinal gradients to form in the MLD depth and strength of the seasonal pycnocline, driven by gradients in incoming irradiance and wind stress. Initially the progression of the bloom is controlled by light availability but the spatial variability of the peak of the bloom is independent of light availability, and is probably controlled by the iron supply.

Acknowledgements

CROZEX was a contribution to the Core Strategic project BICEP (Biophysical Interactions and Control of Export Production) of the National Oceanography Centre, Southampton, funded by the Natural Environment Research Council. Real-time satellite images used during the cruise were supplied by RSDAS from the Remote Sensing Group at PML.

References

Abbott, M.R., 2000. The spring bloom in the Antarctic Polar Front Zone as observed from a mesoscale array of bio-optical sensors. Deep-Sea Research II 47, 3285–3314.

Alonzo, F., Mayzaud, P., Razouls, S., Bocher, P., Cherel, Y., 2003. Seasonal changes in biomass, growth rates and production of subantarctic calanoid copepods in the Bay of Morbihan, Kerguelen Islands. Marine Biology 142, 525–536.

Ansorge, I.J., Froneman, P.W., Pakhomov, E.A., Lutjeharms, J.R.E., Perissinotto, R., van Ballegooyen, R.C., 1999. Physical-biological coupling in the waters surrounding the prince Edward Islands (Southern Ocean). Polar Biology 21, 135–145.

Atkinson, A., Whitehouse, M.J., Priddle, J., Cripps, G.C., Ward, P., Brandon, M.A., 2001. South Georgia, Antarctica: a productive, cold water, pelagic ecosystem. Marine Ecology Progress Series 216, 279–308.

Banse, K., 1996. Low seasonality of low concentrations of surface chlorophyll in the Subantarctic water ring: underwater irradiance, iron or grazing? Progress in Oceanography 37, 241–291.

Blain, S., Treguer, P., Belviso, S., 2001. A biogeochemical study of the island mass effect in the context of the iron hypothesis: Kerguelen Islands, Southern Ocean. Deep-Sea Research I 48, 163–187.

Boyd, P.W., 2002. Environmental factors controlling Phytoplankton Processes in the Southern Ocean. Journal of Phycology 38, 844–861.

Boyd, P.W., LaRoche, J., Gall, M., Frew, R., McKay, R.M.L., 1999. Role of iron, light and silicate in controlling algal biomass in subantarctic waters SE of New Zealand. Journal of Geophysical Research 104 (C6), 13395–13408.

Boyd, P.W., Crossley, A.C., DiTullio, G.R., Griffiths, F.B., Hutchins, D.A., Queguiner, B., Sedwick, P.N., Trull, T., 2001. Control of phytoplankton growth by iron supply and irradiance in the subantarctic Southern Ocean: experimental results from the SAZ Project. Journal of Geophysical Research 106 (C12), 31573–31583.

Boyd, P.W., Watson, A.J., Law, C.S., Abraham, E.R., Trull, T., Murdoch, R., Bakker, D.C.E., Bowie, A., Charette, M., Croot, P., Downing, K., Frew, R., Gall, M., Hadfield, M., Hall, J., Harvey, M., G., J., La Roche, J., Liddicoat, M.R.L., Maldonato, M.T., McKay, R.M.L., Nodder, S., Pickmere, S., Pridmore, R., Rintoul, S.R., Safi, K., Waite, A., Zeldis, J., 2000. A mesoscale phytoplankton bloom in the polar Southern Ocean stimulated by iron fertilization. Nature 407, 695–702.

Bucciarelli, E., Blain, S., Treguer, P., 2001. Iron and manganese in the wake of the Kerguelen Islands (Southern Ocean). Marine Chemistry 73, 21–36.

Campbell, J.W., 1995. The lognormal distribution as a model for bio-optical variability in the sea. Journal of Geophysical Research 100 (C7), 13,237–13,254.

Coale, K.H., Johnson, K.S., Fitzwater, S.E., Gordon, R.M., Tanner, S.J., Chavez, F.P., Ferioli, L., Sakamoto, C., Rogers, P., Millero, F.J., Steinberg, P., Nightingale, P., Cooper, D., Cochlan, W.P., Landry, M.R., Constantinou, J., Rollwagen, G., Trasvina, A., Kudela, R.M., 1996. A massive phytoplankton bloom induced by an ecosystem-scale iron fertilisation experiment in the equatorial Pacific Ocean. Nature 383, 495–501.

Craneguy, P., Park, Y.H., 1999. Topographic control of the Antarctic Circumpolar Current in the south Indian Ocean. C. R. Acad. Sci. Paris, Sciences de la terre et des planetes 328, 583–584.

de Baar, H.J.W., de Jong, J.T.M., Bakker, D.C.E., Loscher, B.M., Veth, C., Bathmann, U.V., Smetacek, V., 1995. Importance of iron for plankton blooms and carbon dioxide drawdown in the Southern Ocean. Nature 373, 412–415.

de Baar, H.J.W., Boyd, P.W., Coale, K.H., Landry, M.R., Tsuda, A., Assmy, P., Bakker, D.C.E., Bozec, Y., Barber, R., Brzezinski, M.A., Buesseler, K.O., Boye, M., Croot, P., Gervais, F., Gorbunov, M.Y., Harrison, P.J., Hiscock, W.T., Laan, P., Lancelot, C., Law, C.S., Levasseur, M., Marchetti, A., Millero, F.J., Nishioka, J., Nojiri, Y., van Oijen, T., Riebesell, U., Rijkenberg, A., Saito, H., Takeda, S., Timmerman, R., Veldhuis, M.J.W., Waite, A.M., Wong, C.S., 2005. Synthesis of iron fertilization experiments: from the Iron Age in the Age of Enlightenment. Journal of Geophysical Research 110(C09S16), doi:10.1029/2004JC002601.

Dierssen, H.M., Smith, R.C., 2000. Bio-optical properties and remote sensing ocean color algorithms for Antarctic Peninsula waters. Journal of Geophysical Research 105 (C11), 26,301–26,312.

Feldman, G.C., McClain, C.R., 2006a. In: Kuring, N., Bailey, S.W. (Eds.), Ocean Color Web, MODIS Reprocessing 1.1, NASA Goddard Space Flight Center. 〈http://oceancolor.gsfc.nasa.gov〉.

Feldman, G.C., McClain, C.R., 2006b. In: Kuring, N., Bailey, S.W. (Eds.), Ocean Color Web, SeaWiFS Reprocessing 5.1, NASA Goddard Space Flight Center. 〈http://oceancolor.gsfc.nasa.gov/〉.

Fielding, S.O., Ward, P., Pollard, R.T., Seeyave, S., Read, J.F., Hughes, J.A., Smith, T., Castellani, C., 2007. Community structure and grazing impact of mesozooplankton during late spring/early summer 2004/2005 in the vicinity of the Crozet Islands (Southern Ocean). Deep-Sea Research II, doi:10.1016/j.dsr2.2007.06.016.

Frost, B.W., 1991. The role of grazing in nutrient-rich areas of the open sea. Limnology and Oceanography 36 (8), 1616–1630.

Gould, J., 2005. A beginners' guide to accessing Argo data. 〈http://www.usgodae.org/argo/argo_data_guide.pdf〉.

Gregg, W.W., Casey, N.W., 2004. Global and regional evaluation of the SeaWiFS chlorophyll data set. Remote Sensing of Environment 93, 463–479.

Holeton, C.L., Nedelec, F., Sanders, R., Brown, L., Moore, C.M., Stevens, D.P., Heywood, K.J., Statham, P.J., Lucas, C.H., 2005. Physiological state of phytoplankton communities in the Southwest Atlantic sector of the Southern Ocean, as measured by fast repetition rate fluorometry. Polar Biology, doi:10.1007/s00300-005-0028-y.

Holm-Hansen, O., Kahru, M., Hewes, C.D., Kawaguchi, S., Kameda, T., Sushin, V.A., Krasovski, I., Priddle, J., Korb, R.E., Hewitt, R.P., Mitchell, B.G., 2004. Temporal and spatial distribution of chlorophyll-*a* in surface waters of the Scotia Sea as determined by both shipboard measurements and satellite data. Deep-Sea Research II 51, 1323–1331.

International Ocean-Colour Coordinating Group, 2000. Remote sensing of ocean colour in coastal, and other optically complex waters. Rep. Int. Ocean-Colour Coord, Group 3, Dartmouth, N.S., Canada.

Johnson, K.S., Gordon, R.M., Coale, K.H., 1997. What controls iron concentrations in the world ocean? Marine Chemistry 57, 137–161.

Korb, R.E., Whitehouse, M.J., 2004. Contrasting primary production regimes around South Georgia, Southern Ocean: large blooms versus high nutrient low chlorophyll waters. Deep-Sea Research I 51, 721–738.

Korb, R.E., Whitehouse, M.J., Ward, P., 2004. SeaWiFS in the Southern Ocean: spatial and temporal variability in phytoplankton biomass around South Georgia. Deep-Sea Research II 51, 99–116.

Landry, M.R., Ondrusek, M.E., Tanner, S.J., Brown, S.L., Constantinou, J., Bidigare, R.R., Coale, K.H., Fitzwater, S.E., 2000. Biological response to iron fertilization in the eastern equatorial Pacific (IronEx II). I. Microplankton community abundances and biomass. Marine Ecology Progress Series 201, 27–42.

Lucas, M., Seeyave, S., Sanders, R., Moore, C.M., Williamson, R., Stinchcombe, M., 2007. Nitrogen uptake responses to a naturally Fe-fertilised phytoplankton bloom during the 2004/2005 CROZEX study. Deep-Sea Research II, doi:10.1016/j.dsr2.2007.06.017.

Maldonato, M.T., Boyd, P.W., Harrison, P.J., Price, N.M., 1999. Co-limitation of phytoplankton growth by light and Fe during winter in the NE subarctic Pacific Ocean. Deep-Sea Research II 46, 2475–2485.

Martin, J.H., Gordon, R.M., Fitzwater, S.E., 1990. Iron in Antarctic waters. Nature 345, 156–158.

Mitchell, B.G., Brody, E.A., Holm-Hansen, O., McClain, C., Bishop, J., 1991. Light limitation of phytoplankton biomass and macronutrient utilization in the Southern Ocean. Limnology and Oceanography 36 (8), 1662–1677.

Moore, J.K., Abbott, M.R., 2000. Phytoplankton chlorophyll distributions and primary productions in the Southern Ocean. Journal of Geophysical Research 105 (12), 28709–28722.

Moore, J.K., Abbott, M.R., Richman, J.G., Smith, W.O., Cowles, T.J., Coale, K.H., Gardner, W.D., Barber, R.T., 1999. SeaWiFS satellite ocean colour data from the Southern Ocean. Geophysical Research Letters 26 (10), 1465–1468.

Moore, C.M., Seeyave, S., Hickman, A.E., Allen, J.T., Lucas, M.I., Planquette, H., Pollard, R.T., Poulton, A.J., 2007. Iron-light interactions during the CROZet natural iron bloom and EXport experiment (CROZEX) I: Phytoplankton growth and photophysiology. Deep-Sea Research II, doi:10.1016/j.dsr2.2007.06.011.

O'Reilly, J.E., Maritorena, S., Mitchell, B.G., Siegel, D.A., Carder, K.L., Garver, S.A., Kahru, M., McClain, C., 1998. Ocean color chlorophyll algorithms for SeaWiFS. Journal of Geophysical Research 103 (C11), 24,937–24,953.

Park, Y.H., Gamberoni, L., Charriaud, E., 1993. Frontal structure, water masses, and circulation in the Crozet Basin. Journal of Geophysical Research 98 (7), 12361–12385.

Planquette, H.F., Statham, P.J., Fones, G.R., Charette, M.A., Moore, C.M., Salter, I., Nédélec, F.H., Taylor, S.L., French, M., Baker, A.R., Mahowald, N., Jickells, T.D., 2007. Dissolved iron in the vicinity the Crozet Islands, Southern Ocean. Deep-Sea Research II, doi:10.1016/j.dsr2.2007.06.019.

Pollard, R.T., Read, J.F., 2001. Circulation pathways and transports of the Southern ocean in the vicinity of the Southwest Indian Ridge. Journal of Geophysical Research 106 (2), 2881–2898.

Pollard, R.T., Sanders, R., 2006. RRS Discovery cruises 285/286, 3 November–10 December 2004, 13 December 2004–21 January 2005; CROZet circulation, iron fertilization and EXport production experiment (CROZEX), 260pp, Southampton Oceanography Centre, Cruise Report No. 60.

Pollard, R.T., Lucas, M.I., Read, J.F., 2002. Physical controls on biogeochemical zonation in the Southern Ocean. Deep-Sea Research II 49, 3289–3305.

Pollard, R.T., Venables, H.J., Read, J.F., Allen, J.T., 2007. Large scale circulation around the Crozet Plateau controls an annual phytoplankton bloom in the Crozet Basin. Deep-Sea Research II, doi:10.1016/j.dsr2.2007.06.012.

Razouls, S., Koubbi, P., Mayzaud, P., 1996. Spatio-temporal distribution of mesozooplankton in a sub-Antarctic coastal basin of the Kerguelen Archipelago (southern Indian Ocean). Polar Biology 16, 581–587.

Razouls, S., Du Reau, G., Guillot, P., Maison, J., Jeandel, C., 1998. Seasonal abundance of copepod assemblages and grazing pressure in the Kerguelen Island area (Southern Ocean). Journal of Plankton Research 20 (8), 1599–1614.

Ryabchenko, V.A., Fasham, M.J.R., Kagan, B.A., Popova, E.E., 1997. What causes short-term oscillations in ecosystem models of the ocean mixed layer. Journal of Marine Systems 13, 33–50.

Sandwell, D.T., Smith, W.H.F., 1997. Marine gravity anomaly from Geosat and ERS1 satellite altimetry. Journal of Geophysical Research 102 (5), 10039–10054.

Sedwick, P.N., Blain, S., Queguiner, B., Griffiths, F.B., Fiala, M., Bucciarelli, E., Denis, M., 2002. Resource limitation of phytoplankton growth in the Crozet Basin, Subantarctic Southern Ocean. Deep-Sea Research II 49, 3327–3349.

Seeyave, S., Lucas, M.I., Moore, C.M., Poulton, A.J., 2007. Phytoplankton productivity and community structure in the vicinity of the Crozet Plateau during austral summer 2004/2005. Deep-Sea Research II, doi:10.1016/j.dsr2.2007.06.010.

Sunda, W.G., Huntsman, S.A., 1997. Interrelated influence of iron, light and cell size on marine phytoplankton growth. Nature 390, 389–392.

Timmermans, K.R., Gerringa, L.J.A., de Baar, H.J.W., van der Wagt, B., Veldhuis, M.J.W., de Jong, J.T.M., Croot, P., 2001. Growth rates of large and small Southern Ocean diatoms in relation to availability of iron in natural seawater. Limnology and Oceanography 46 (2), 260–266.

Welschmeyer, N.A., 1994. Fluorometric analysis of chlorophyll *a* in the presence of chlorophyll *b* and Pheopigments. Limnology and Oceanography 39 (8), 1985–1992.

Wolff, G., 2006. Initial Cruise Report. D300 Bentic CROZET. 1st December 2005–14th January 2006. 139pp. 〈http://www.bodc.ac.uk/data/information_and_inventories/cruise_inventory/report/d300.pdf〉.